Available online at www.sciencedirect.com
ScienceDirect
Journal of Power Sources 179 (2008) 584–591
JOURNAL OF POWER SOURCES
www.elsevier.com/locate/jpowsour

Development of a PEM stack and performance analysis including the effects of water content in the membrane and cooling method

Yong Hun Park [a,*], Jerald A. Caton [b]

[a] *Arbin Instruments, 762 Peach Creek Cut Off Road, College Station, TX 77845, United States*
[b] *E^3 (Engines, Emissions, Energy) Laboratory, Mechanical Engineering, Texas A&M University, College Station, TX 77843-3123, United States*

Received 18 December 2007; received in revised form 24 January 2008; accepted 25 January 2008
Available online 6 February 2008

Abstract

For the use of proton exchange membrane (PEM) fuel cell systems to become widespread, the components required to build one should be minimized. Because a PEM fuel cell has a limited operating temperature range, it requires some kind of cooling method. In this study, different cooling methods were investigated experimentally. A PEM fuel cell stack with an active area of 100 cm^2 and 8 cells in series was developed and used in this research. When 50% relative humidity inlet gases were supplied (at 15 A of current discharge and 70 °C), cell temperatures at the center increased from around 60 °C to 85 °C, and cell voltage dropped from 4.8 V to 3.2 V because of membrane drying (insufficient cooling). When fully hydrated inlet gases (100% relative humidity) were supplied to the PEM stack at the same test conditions, the cell temperature remained around 65 °C, and stack voltage remained around 5.7 V at 15 A of current discharge. Fully hydrated inlet gases play a positive role both for water transport (when the proton moves from the anode to the cathode) and to maintain the fuel cell stack temperature to prevent stack drying.

Keywords: PEM fuel cell; Stack; Performance; Thermal management; Cooling method

1. Introduction

One of the main attractions of fuel cells relative to the internal combustion engine (or power sources using any hydrocarbon fuel) is the potential to produce power with minimal or zero emissions. Therefore, attention to fuel cell technology has increased due to environmental concerns such as global warming and the limitation of oil sources. Although many areas have been studied and developed to commercialize fuel cells, simplifying the overall fuel cell system will shorten the time of development. The polymer electrolyte membrane (PEM) fuel cell system includes the PEM fuel cell stack, gas supplying systems, a humidifier system, an exhaust system, a cooling system, and so on. Because heat is generated during the electrochemical reactions, thermal management is essential for long-term operation and durability.

1.1. Literature review

The flow field structure is one of the factors that influences fuel cell performance. It is related mainly to water management because water is generated by the chemical reaction in the cell. Three different flow types (co-flow, cross-flow, and counter flow) were tested by Scholta et al. [1]. Their results showed the dependence of cell performance on flow direction for co-flow and counter flow systems. The maximum power density obtained was about 0.32 mW cm^{-2} and 0.42 mW cm^{-2} for the co-flow and counter flow designs, respectively [1]. The cross-flow performance was between the co-flow and counter flow designs [1]. In the study described in this paper, the counter flow design was adopted and used for a PEM fuel cell stack.

Hwang and Hwang published a parametric study of a double-cell stack of PEM fuel cells [2]. Their study included the effects of cell operating temperature, the dew point of reactants, channel flow back-pressure, and flow channel dimensions. When the fuel cell operating temperature was 30 °C, the effect of the dew point of the reactants was insignificant [2]. However, increas-

* Corresponding author. Tel.: +1 979 690 2751.
E-mail address: park00@gmail.com (Y.H. Park).

0378-7753/$ – see front matter © 2008 Elsevier B.V. All rights reserved.
doi:10.1016/j.jpowsour.2008.01.050

ing the cell's operating temperature to 80 °C caused membrane dehydration and decreased cell performance [2]. In their study, cell performance with membrane dehydration depended on the cooling method. Hwang and Hwang [2] studied the effect of the channel dimension on cell performance. The widths varied: 3.0 mm, 2.5 mm, 2.0 mm, and 1.5 mm. When the narrowest width was used, cell performance increased significantly because it minimized the diffusion pathway [2].

The channel depth effect on the performance of a fuel cell was studied by Park and Caton [3]. The shallow flow field design dramatically influenced the performance of an air-breathing fuel cell at low relative humidity and slightly affected performance at high relative humidity. Using information from both Hwang and Hwang [2] and Park and Caton [3], the channel depth and width of the flow field for the current research were set at 0.6 mm and 0.9 mm, respectively.

Qi and Kaufman investigated a double-path-type 4-cell PEM fuel cell stack with an active area of 27.6 cm^2 for its performance under dry-reactant conditions [4]. Their stack had two gas inlets and two gas outlets that were adjacent to one another with reactant flowing in opposite directions. The water produced was used to hydrate the membrane and catalyst layers. The exiting moist gas hydrated the dry, entering gas [4]. After the stack had generated 6 A for 2 h, the stack voltage declined quickly and stabilized at 1.7 V (where the current was less than 1 A), which was proof of a drying stack. Because no humidity was added to the inlet gases, the produced water was the only source for the electro-osmotic drag, and that was insufficient. When no humidified gas was supplied, the current that the fuel cell could discharge and maintain was limited to a very low current density. Nonetheless, this design was a good approach for cases not using an external humidifier.

Rodatz et al. [5] investigated some critical aspects of large fuel cell stacks, such as the supply system, stack failures, and voltage stability. Uniform distribution of the reactant gases to many channels was hard to achieve. When the discharged current change was very fast compared to the response of the reactant supply system, undersupply and negative voltage could occur. When monitoring the stack voltage, researchers could not record the voltage drop of a single cell. A solution by Rodatz et al. [5] was to monitor the voltage of every cell or at least a small group of cells. Another failure was a leak in the membrane caused by either mechanical stress or hot spots. The generation of large amounts of heat resulted in an increase in the membrane resistance, which formed hot spots in the membrane. The third failure was overheating of the fuel cell stack, which led to severe dehydration of the membrane, resulting in a large resistance and performance loss. To prevent overheating, a sufficient cooling flow should be used at all times. A large pressure difference across the membrane between the reactant gases was one of the reasons for the hot spot in the membrane, which resulted in direct mixing of hydrogen and air. To prevent this problem, pressure relief valves were installed, and pressure controllers were used to avoid large pressure differences [5].

Eckl et al. [6] experimented with water management for a fuel cell. They studied two scenarios: (1) drying out and (2) flooding. Their results showed cell voltages as functions of current and testing time. For the drying out scenario, when stack cooling was off, stack temperature increased. Because the stack had 20 cells, the cells at the center, such as #9, #10, and #11, had a sharp drop in voltage from both local overheating and dehydration.

In the current study, a PEM stack (100 cm^2 active area and 8 cells in series) was designed, and its performance related to the water content in the membrane, the cooling method, and the assembly pressure.

2. Experimental setup

The next subsections will describe the testing system, MEA preparation, flow field design, and specifications and preparations of the PEM fuel cell stack used in this research.

2.1. Overview of the fuel cell testing system

In this research, a hydrogen generator supplied hydrogen to the fuel cell, which led to the elimination of hydrogen cylinders. City water was supplied to a de-ionized (DI) water filtering system. The produced DI water was fed to the hydrogen generator. Chilled water was used to control the temperature of the dew point humidifier (DPH). The chilled water also decreased the temperature of the exhaust gas for water removal. The de-ionized water for humidifying was refilled automatically using an automatic level control. The delivery of the gases from the supply to the internal gas line was controlled by a pressure regulator. This regulator reduced the pressure from the inlet pressure to the inline pressure. From the pressure regulator, the delivery of the gases was controlled by electronic mass flow controllers (MFCs), check valves, and solenoid valves. The gas went through the humidifier and heated exit-pipe to the fuel cell. The MFCs were powered and controlled by a flow control board in the computer-controlled module of the testing system. Solenoid valves were all powered by 24 VDC from the local power supply. Further details of the testing system can be found elsewhere [3].

2.2. Membrane and electrode assembly (MEA) preparation

The active area of the membrane electrode assembly (MEA) was 100 cm^2. E-TEK ELAT electrodes were used for both the anode and the cathode. The average Pt loading was 0.57 mg cm^{-2} on both the cathode and anode sides. As an initial start-up procedure, the MEA was operated at 25 °C with H_2 at 1.2 stoichiometric and air at 3 stoichiometric flow rates. For this procedure, the fuel cell voltage was constant at 0.2 V as the cell temperature was raised to 60 °C. After reaching this temperature, the cell voltage cycled between 0.2 V and 0.6 V at an interval of 20 min for several hours until the cell performance stabilized.

2.3. Flow field design

The shape, size, and pattern of the flow channels can significantly affect the performance of a fuel cell. Choosing the right flow pattern is especially critical for a PEM fuel cell. Although

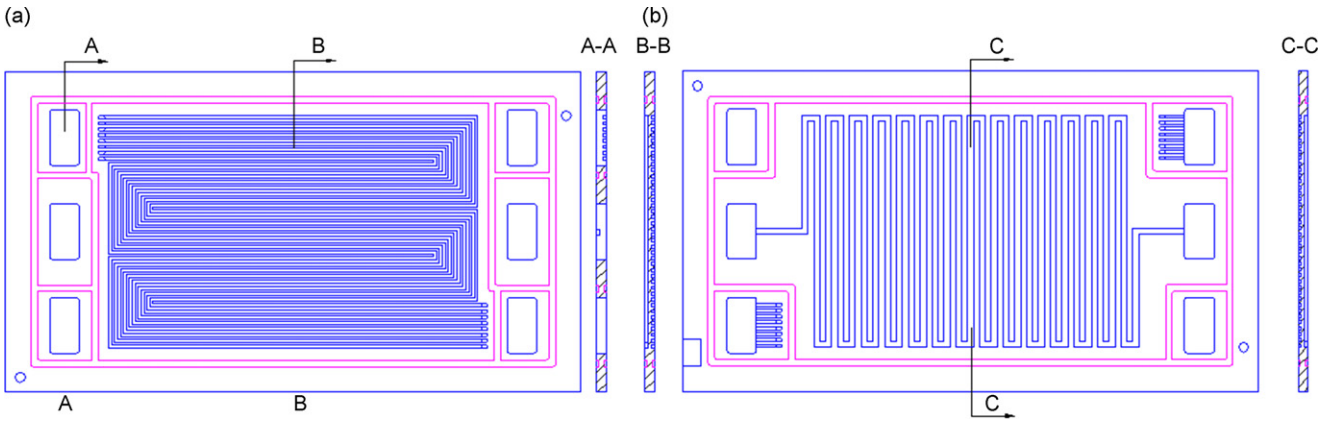

Fig. 1. Schematic of a bipolar plate used in this research: (a) front side of bipolar plate, (b) back side of bipolar plate.

research groups and developers have used a wide variety of flow patterns, the most basic patterns are parallel, serpentine, parallel serpentine, and interdigited.

The major advantage of a parallel configuration is the low pressure-drop between the gas inlet and outlet; disadvantages include the fact that the flow distribution may not be uniform. For a serpentine flow, the advantage is the capability for water removal. Because only one flow path exists in the pattern, liquid water is forced to exit the channel. But large-area fuel cells cause a large pressure-drop in this configuration. With an interdigited flow pattern, the advantage is the forced convection of the reactant gases through the gas diffusion layers. A hybrid design with 8 serpentine flow channels, combining the advantages of the serpentine and parallel patterns was selected for this study. The channel depth, width, and landing were 0.06 cm, 0.11 cm, and 0.09 cm, respectively. The cooling channel depth, width, and landing were 0.1 cm, 0.2 cm, and 0.2 cm, respectively. Table 1 lists the specifications of a bipolar plate.

2.4. Stack preparation

Fig. 1(a) and (b) shows the field design for reactant gases such as air and hydrogen in the coolant flow field. Fig. 2 shows a schematic of the fuel cell stack used in this research, which included end plates, conduction plates, bipolar plates, and MEA. Fig. 3(a) shows the assembled PEM fuel cell stack used in this research. It has 100 cm^2 of active area in an 8-cell series. Compression pressure was applied to seal the MEAs and polar plates and create good contact between them and good performance of the MEAs. A synthetic graphite material with high electric

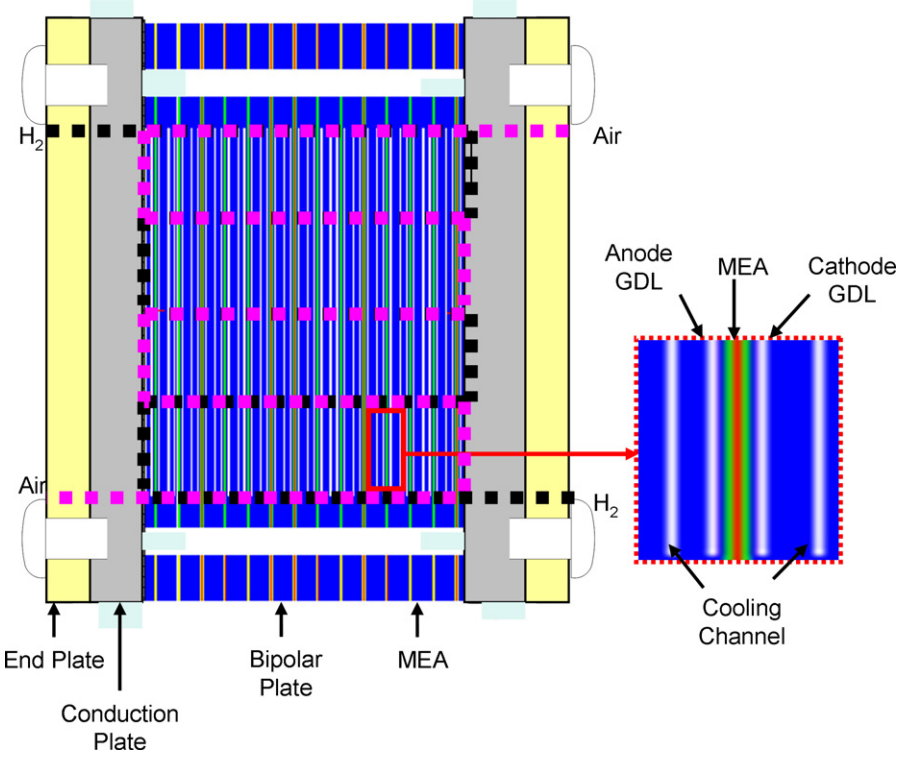

Fig. 2. Schematic of the PEM fuel cell stack with 8 series cells.

Table 1
Specification of a bipolar plate for a 250 W PEM fuel cell stack

Item	Illustration
Active area (cm^2)	100
Bipolar plate area ($W \times H$)	19.5 cm × 10.9 cm
Bipolar plate thickness (cm)	0.318
Cell number	8
Channel depth (cm)	0.06
Channel width (cm)	0.11
Channels landing (cm)	0.09
Cooling channel deep (cm)	0.1
Cooling channel width (cm)	0.2
Cooling channel landing (cm)	0.2
Flow field type (serpentines)	8

conductivity and high temperature resistance was used for the bipolar plate. Fig. 3(b) shows the front and back of the anode and cathode graphite plates, which have flow fields for each gas (hydrogen, air) at the front and coolant at the back. These graphite plates included the standard 8 serpentine flow channels. When making the series stack, a cooling chamber was put between each anode and cathode flow field, which provided good heat transfer from reactants to coolant. Thermocouples were inserted into the #2, #4, #6, and #7 positions to measure the temperatures. Fig. 3(c) shows the general experimental setup, which included a stack of 8 PEM fuel cells in series, pressure sensors to measure pressure variation, thermocouples to measure the temperature of the graphite plates, and auxiliary voltage connections to measure each cell's voltage.

3. Result and discussion

The results are presented in three sections: (1) effect of cooling in the stack, (2) effect of water content in the membrane in the stack, and (3) effect of assembly pressure for the stack.

3.1. Effect of cooling in the PEM stack

Fig. 4(a) shows the individual cell voltages corresponding to cases with a constant 15 A (2 h), 20 A (1 h), and 10 A (1.5 h) when the temperature of the inlet gases was 70 °C and the relative humidity was 80% without any cooling. For the first 2 h, the current discharged from the fuel cell stack was set at 15 A. The voltage for each cell was maintained around 0.5 V and increased a little with increasing test times. At 15 A, 0.15 A cm^{-2}, the heat released during electrochemical reactions was not high enough to make the fuel cell stack suffer from drying. In this case, the generated water led to enhanced proton transport from the anode to the cathode. When the current discharge was set at 20 A and maintained for 1 h, the voltage from each cell dropped from about 0.5 V to as low as about 0.2 V. The cells at the center of the fuel cell stack, #4, #5, and #6, had the sharpest drops in voltage. At a discharge current of 10 A for one and a half hours, the voltage for each cell recovered to about 0.7 V.

Fig. 4(b) shows the cell temperatures (#2 cathode, #4 anode, #6 cathode, and #7 anode) corresponding with a constant 15 A (2 h), 20 A (1 h), and 10 A (1.5 h) (this result was obtained at the same time as Fig. 4(a)). For the first 2 h at 15 A, cell temperatures were around 80 °C. When the discharge current was set at 20 A, cell temperatures increased to 90–100 °C. Because no thermal management was used during the electrochemical reactions, the stack generated heat. This case resulted in a sharp drop in cell voltage as shown in Fig. 4(a). The cell at the #4 anode had the highest temperature increase.

One way to measure internal resistance in an operational fuel cell is the current interrupt method, which measures internal resistances. As shown in Fig. 4(c), internal resistances remained around 0.2 Ω cm^2 for the first 2 h when the fuel cell stack discharged 15 A. When the fuel cell stack discharged 20 A, cell temperature increased dramatically, which led to an increase

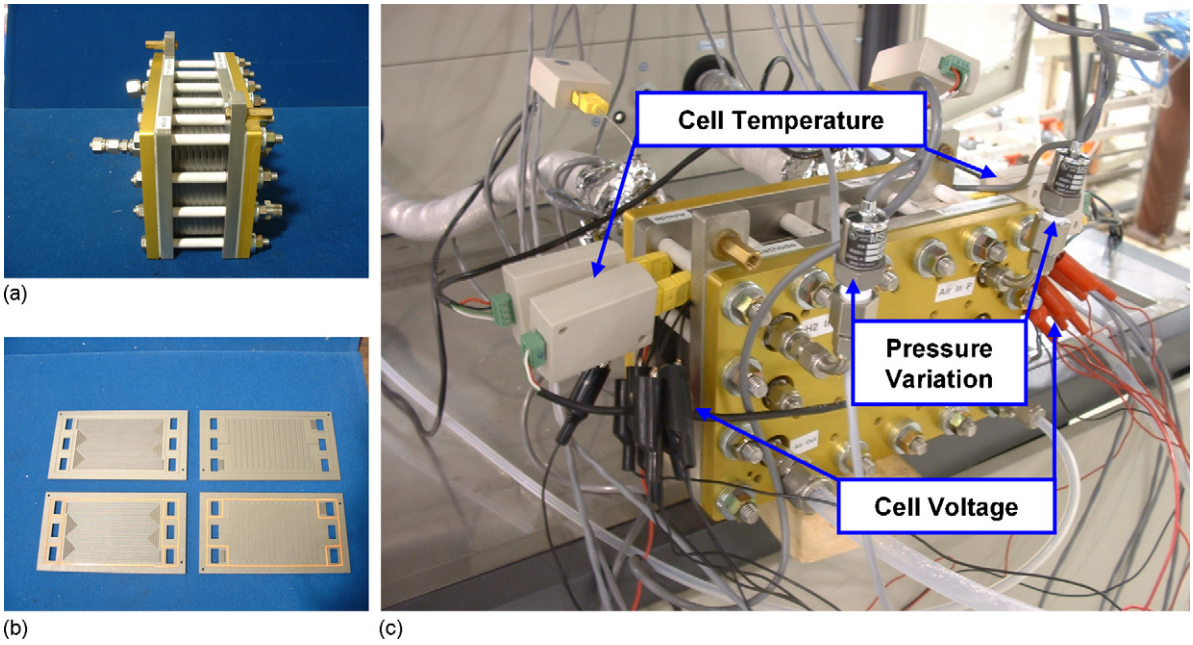

Fig. 3. (a) PEM fuel cell stack used in this study, (b) bipolar graphite plates, and (c) testing setup of PEM fuel cell stack.

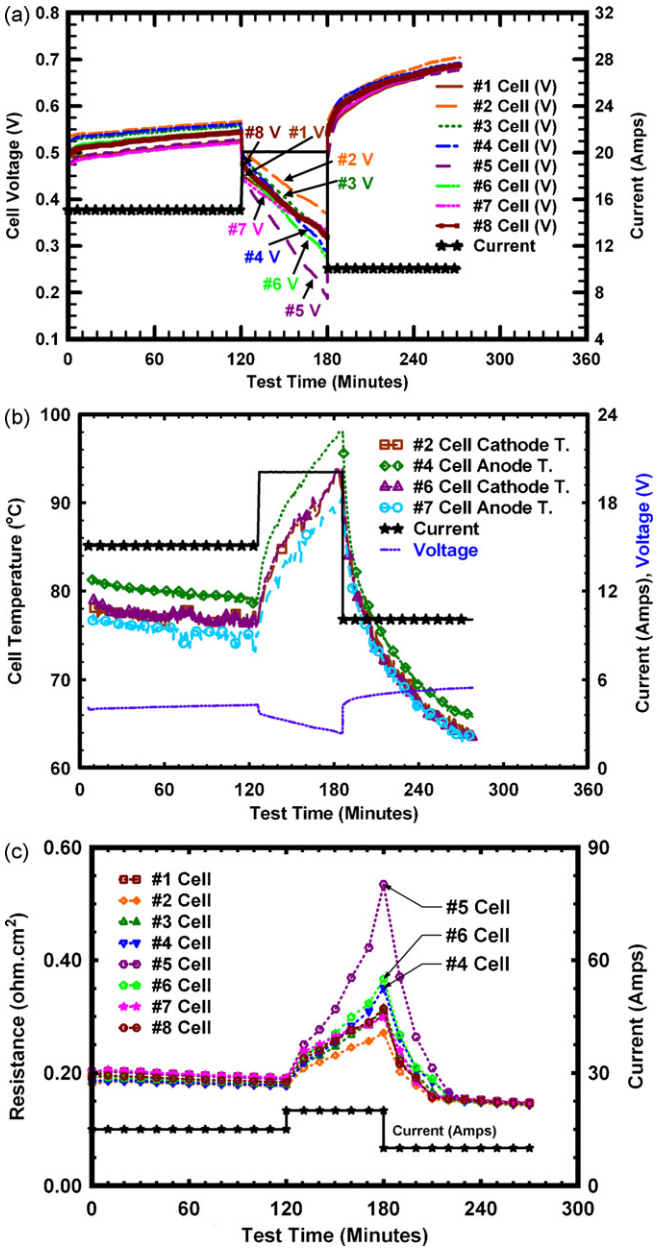

Fig. 4. (a) Each cell voltages, (b) cell temperatures and stack voltage, (c) internal resistance, corresponding with constant current 15 A (2 h), 20 A (1 h), and 10 A (1.5 h). Temperature = 70 °C, relative humidity of the inlet gases = 80%, and no cooling method used.

in the internal resistance. The #5 cell at the center obtained the highest internal resistance, up to around 0.55 Ω cm^2. As the membrane dried and the temperature increased, proton conductivity gradually reduced.

Fig. 5(a) shows the stack voltage and discharged current (open circuit voltage and 15 A) as functions of time. As an operation schedule, the open circuit voltage was measured for 1 h to stabilize the relative humidity of the inlet gases, which was set to 50%. After 1 h, the fuel cell stack discharged 15 A while the relative humidity of the inlet gases was maintained at 50% for 1 h. After that, the relative humidity of the inlet gases was increased from 50% to 100%. At that point, the fuel cell stack had discharged 15 A for 1 h and 40 min. Ambient air was supplied to the coolant channel using a compressor, and a fan was used to cool down the stack. With the same operating conditions (except for the relative humidity of the inlet gases), the obtained stack voltages were much different. For the case with 50% relative humidity, the stack voltage dropped from around 4.7 V to 3.0 V for 1 h. For the case with 100% relative humidity, however, the stack voltage maintained around 5.7 V for 1 h and decreased a little after that. The voltage drop for the cases with 50% relative humidity of the inlet gases shown in Fig. 5(a) is related to the drying operating conditions.

To check whether the stack suffered from drying, cell temperatures at #2 cathode, #4 anode, #6 cathode, and #7 anode were

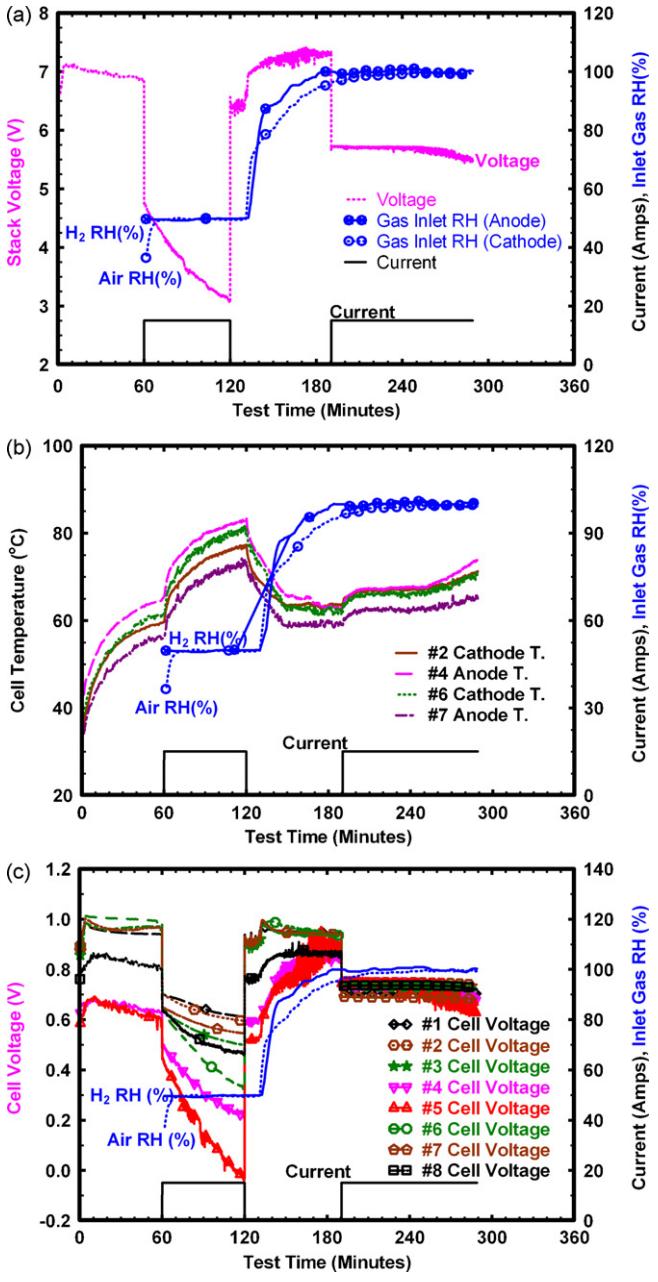

Fig. 5. (a) Stack voltage, (b) cell temperatures variation, (c) cell voltages, as a function of current with different inlet gases' relative humidity (50% and 100%). Temperature = 70 °C, air cooling through cooling channels used.

measured (Fig. 5(b)). When the current discharged 15 A, cell temperatures increased from around 60 °C to 80 °C. When gases with 100% relative humidity were supplied, however, the cell temperatures remained around 65 °C for 1 h and then increased a little to 70 °C. As illustrated by these results, supplying fully hydrated inlet gases enabled the protons to move easily from the anode to the cathode and also helped the fuel cell stack maintain its operating temperature.

The number of cells in the stack and operating current density are two of the most critical parameters for thermal management. Increasing either of these factors results in a significant increase in the overall stack temperature gradient. Cell temperatures increase from 40 °C to 60 °C in the initial hour under the open circuit voltage (OCV) condition shown in Fig. 5(b). The temperature of the inlet gases supplied to the fuel cell stack was set to 70 °C. As time went on, the inlet gases warmed up the MEA and graphite plates, as well. A higher inlet temperature leads to a higher average stack temperature. Inlet gases act as a coolant to keep the fuel cell stack temperature in a good operating range. The inlet volumetric flow rate and the ratio between the active area and the nominal stack cross-sectional area are other factors that determine the stack temperature under the OCV condition.

Fig. 5(c) shows the individual cell voltages and discharged current (open circuit voltage and 15 A) at the same time shown in Fig. 5(a) and (b). The cells around the center (#4, #5, and #6 cells) had a sharper drop in voltage at 15 A discharge current when gases at 50% relative humidity were supplied than the cells at the sides (#1, #2, #3, #7, and #8 cells). When the relative humidity of the inlet gases increased to 100%, each cell obtained around 0.7 V, regardless of where it was located. Increasing the relative humidity of the inlet gases from 50% to 100%, therefore, provided conditions for easy proton transport and maintained stack temperatures, as well.

Fig. 6 shows the voltage, power, and current fixed at 30 A when the inlet gases were 70 °C with a relative humidity of 100%. Two cases (no cooling method and compressed air supplied to the cooling channel) were studied. After the test started, the fuel cell stack obtained around 4.8 V for both cases (no cooling and air cooling). When no cooling method was used, the fuel cell stack voltage dropped to 3.0 V, and power dropped to 90 W

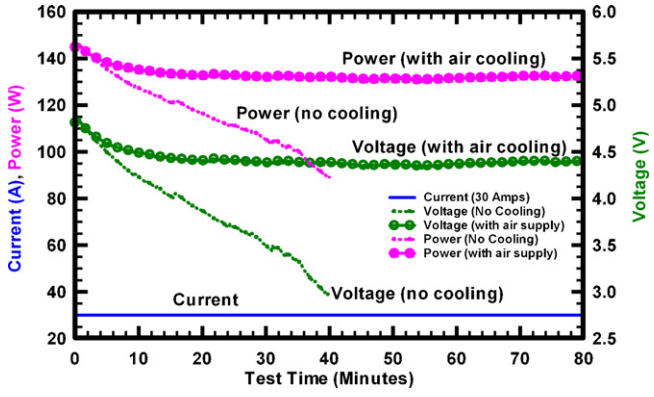

Fig. 6. Voltage and power at fixed 30 A when the inlet gases were 70 °C and the relative humidity of the inlet gases were 100% with air cooling and no cooling.

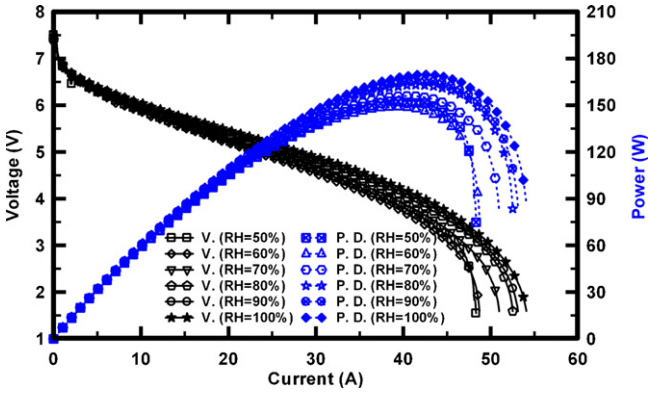

Fig. 7. Stack voltage and power as a function of current at 70 °C with fan cooling.

after 40 min. Using the air-cooling method through the cooling channels, the voltage remained at 4.4 V, which obtained 140 W. Without a complex water (or coolant) cooling method, which should include temperature response feedback (heat exchanger, heating, and cooling system), supplying compressed ambient air to the cooling channel and fully humidified (100% relative humidity) reactant gases enabled maintenance of the fuel cell stack temperature and power below/at 0.3 A cm^{-2}. However, in high current density regions, proper thermal management using a cooling system with temperature feedback should be applied to operate a PEM fuel cell stack.

3.2. *Effect of water content in the membrane*

As shown in the previous section, the level of the inlet gases' relative humidity plays a role in water transport in the membrane and is related to thermal management in a fuel cell stack.

Fig. 7 shows voltage and power as a function of current with differing relative humidity of the inlet gases. Because this stack had 8 cells in series, the open circuit voltage reached around 7.5 V. The maximum power obtained varied from 150 W to 170 W when the relative humidity of the inlet gases varied from 50% to 100%, respectively. These voltages and powers as a function of current were obtained using fans outside the stack without any cooling medium through the cooling channel.

Fig. 8(a) shows the cell voltages as a function of the discharged current when the temperature of the inlet gases was 70 °C and the relative humidity was 80% with fan cooling. The cells around the center of the fuel cell stack (#4, #5, and #6) had a voltage drop after 30 A, which resulted from drying and overheating because no cooling medium was supplied to the stack.

Fig. 8(b) shows the cell voltages as a function of the discharged current when the temperature of the inlet gases was 70 °C and the relative humidity was 90% with fan cooling. Fig. 8(c) shows cell voltages as a function of the discharged current when the temperature of the inlet gases was 70 °C and the relative humidity was 100% with fan cooling. As seen in all Fig. 8(a)–(c), cell voltages at cells #1, #2, and #3 obtained much higher values than other cells, especially for high currents. Because the inlet gases are supplied through one inlet, the hydro-

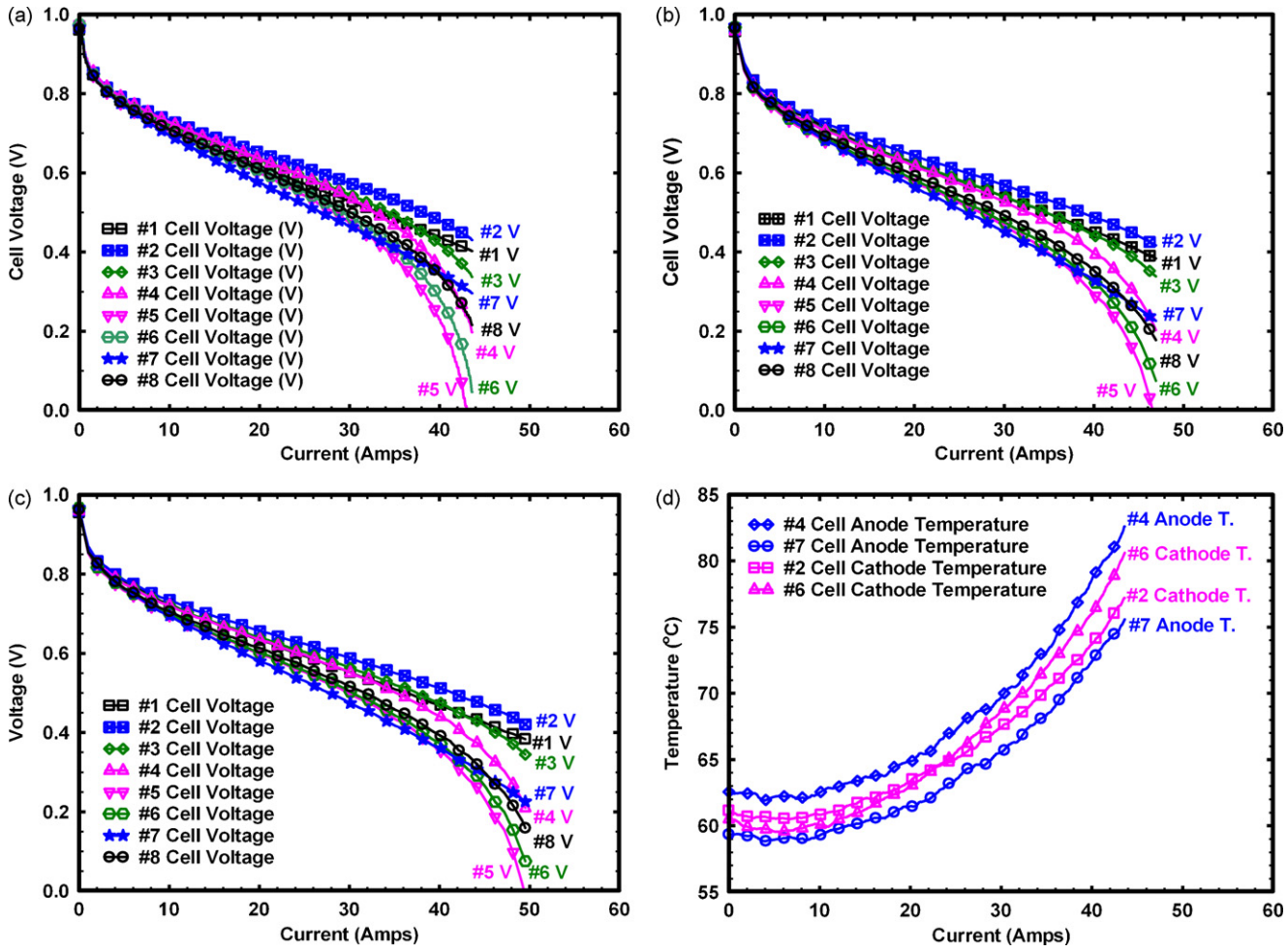

Fig. 8. Cell voltages as a function of the discharged current with (a) 80% relative humidified gases, (b) 90% relative humidified gases, (c) 100% relative humidified gases, (d) cell temperatures as a function of the discharge current. The temperature of the inlet gases were 70 °C with fan cooling.

gen and air seemed to suffer from unequal distribution. If cell voltages had suffered from overheating, the cells at the other side (#7 and #8) should have had higher voltages. Cells #7 and #8 lacked sufficient inlet gases, and the voltage drop at cells #4, #5, and #6 resulted from overheating. Equal distribution of inlet gases to a fuel cell stack is left for future work. Fig. 8(d) shows cell temperatures as a function of the discharged current. Those temperatures were recorded at the same time as the polarization cycles shown in Fig. 8(a). At low current density, the cell temperature did not increase much and remained steady. At high current density, the cell temperature increased sharply, which led to performance decreases.

Cell voltages as a function of the discharged current shown in Fig. 8(a)–(c) were obtained after the relative humidity and temperature of the inlet gases reached set points (80%, 90%, and 100% at 70 °C). However, cell voltages as a function of the discharged current shown in Fig. 5(c) were measured when the inlet gases were set to 70 °C with no humidifying for 1 h. The cells that suffered from dry operation had lower open circuit voltage unless they recovered.

The cells near the center of the stack (#4, #5, and #6) yielded an early voltage drop as a result of the drying and overheating, particularly at high current densities, which could be evidenced by the measured cell temperatures shown in Fig. 8(d). However, cells #1 and #2 exhibited higher cell voltages than cells #7 and #8, as shown in Fig. 8(a)–(c). Those differences resulted from unequal flow distribution. Even though external manifolds ensure uniformity, internal manifolds were used for better sealing. Another explanation is that in the "U"-shape stack flow configurations used for this PEM stack, cell #1 is nearest to the inlet gases. Using a "Z"-shape stack flow configuration and external manifold are left for future study.

Fig. 9 shows the voltage and average stack temperature as a function of time for these inlet gases' relative humidity levels at a constant 25 A. Fans were used to reduce the stack temperature for the cases in Fig. 9. When the relative humidity of the inlet gases varied to 80%, 90%, and 100%, the stack voltage dropped for 20 min from around 4.6 V to 3.7 V, from 4.5 V to 4.0 V, and from 4.6 V to 4.2 V, respectively. In the meantime, the average stack temperatures increased from 64 °C to 83 °C, from 74 °C to 83 °C, and from 75 °C to 85 °C, respectively. When compressed ambient air was supplied to the coolant channel for the stack, as shown in Fig. 6, the stack voltage maintained 4.4 V after 10 min of operation. As shown in

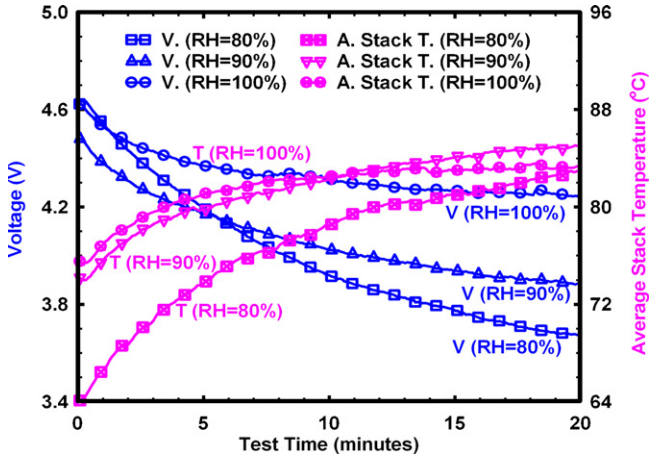

Fig. 9. Voltage at constant current 25 A with fan cooling at 70 °C.

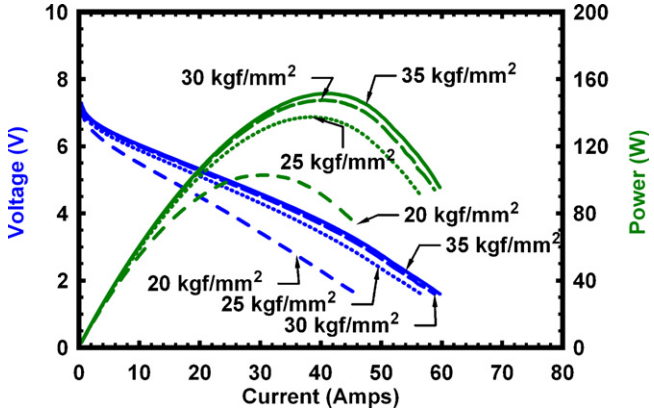

Fig. 10. Voltage and power as a function of current with different assembly pressures.

Fig. 9, using fans outside the stack was insufficient to maintain the operating temperature and voltage for a 250 W fuel cell stack.

3.3. Effect of assembly pressure

When a fuel cell stack is assembled with insufficient pressure, it can lead to leakage of fuels and create a high contact resistance. If a stack has too much pressure, it can damage the gas diffusion layer and/or the MEA. Uneven distribution of contact pressure will result in hot spots, which can shorten fuel cell life. Five different assembly pressures – 20, 25, 30, 35, and 40 kgf mm^{-2} – were selected for this study. Fig. 10 shows the voltage and power density of the fuel cell stack as a function of current density with different assembly pressures. When the assembly pressure was 20 kgf mm^{-2}, the maximum power obtained was around 100 W. When the assembly pressure increased to 25 kgf mm^{-2}, 30 kgf mm^{-2}, and 35 kgf mm^{-2}, the obtained maximum powers increased to 135 W, 150 W, and 152 W, respectively. When the assembly pressure went to 40 kgf mm^{-2}, some cracks were found in the gas diffusion layer.

4. Conclusions

A PEM fuel cell stack (8 cells in series and 100 cm^2 active area) was developed and used in this research to study water content, cooling methods, and assembly pressure. Because heat must be generated during electrochemical reactions, a cooling method should be used to maintain fuel cell temperature, performance, and lifespan. However, a cooling method adds complexity to a fuel cell system. In this study, simple cooling methods such as supplying fully hydrated gases and using compressed air through the cooling channel were examined. Also, the effects of water content in the membrane were studied. Specific conclusions and findings include:

- Below 0.2 A cm^{-2} of current density, the fuel cell stack (8 cells in series and 100 cm^2 active area) supplied with gases at 80% relative humidity maintained its operating temperature without any cooling method. The generated water permitted high voltage at a fixed current density without any voltage drop. At more than 0.2 A cm^{-2} of current density, the fuel cell stack supplied with gases at 80% relative humidity needed cooling to maintain its cell temperatures.
- At 0.3 A cm^{-2} of current density, the fuel cell stack (8 cells in series and 100 cm^2 active area) supplied with gases at 100% relative humidity and using air cooling through the cooling channels maintained its power around 140 W. However, without air cooling at 0.3 A cm^{-2} of current density, the stack showed a sharp drop of power from 150 to 90 W after 40 min of operation.
- When the fuel cell stack suffered from drying, stack temperature increased at fixed current density. When fully hydrated gases (100% relative humidity) were supplied to the fuel cell stack, the easy transport of protons from the anode to the cathode maintained fuel cell stack temperatures and prevented the stack from drying.
- Among different assembly pressures (20, 25, 30, 35, and 40 kgf mm^{-2}), 35 kgf mm^{-2} with 100 cm^2 active area had the highest power without showing cracks in the gas diffusion layer.

References

[1] J. Scholta, F. Haussler, W. Zhang, L. Kuppers, L. Jorissen, W. Lehnert, J. Power Sources 155 (2006) 60–65.
[2] J. Hwang, H. Hwang, J. Power Sources 104 (2002) 24–32.
[3] Y.H. Park, J.A. Caton, J. Fuel Cell Sci. Technol., Paper No: FC-07-1114, in press.
[4] Z. Qi, A. Kaufman, J. Power Sources 109 (2002) 469–476.
[5] P. Rodatz, F. Buchi, C. Onder, L. Guzzella, J. Power Sources 128 (2004) 208–217.
[6] R. Eckl, W. Zehtner, C. Leu, U. Wagner, J. Power Sources 138 (2004) 137–144.